european burn journal

MDPI

Article

NaHS-Hydrogel and Encapsulated Adipose-Derived Stem Cell Evaluation on an Ex Vivo Second-Degree Burn Model

Lucille Capin [1,2,3,*,†], Olivia Gross-Amat [1,2,3,*,†], Marie Calteau [2], Marie-Rose Rovere [2], Damien Salmon [4] and Céline Auxenfans [2,5]

1 Lyon-Est School of Medicine, University Claude Bernard Lyon-1, 69100 Villeurbanne, France
2 Bank of Tissues and Cells, Lyon University Hospital (Hospices Civils de Lyon), 69003 Lyon, France; calteaumarie@yahoo.fr (M.C.); rovere_marierose@hotmail.com (M.-R.R.); celine.auxenfans@chu-lyon.fr (C.A.)
3 CarMeN Laboratory, INSERM U1060, INRA U1397, INSA de Lyon, 69600 Oullins, France
4 Fundamental, Clinical and Therapeutic Aspects of Skin Barrier Function, EA4169, University of Lyon 1, 69008 Lyon, France; salmondam@hotmail.fr
5 Tissue Biology and Therapeutic Engineering Laboratory, UMR 5305, 69007 Lyon, France
* Correspondence: lucille.capin@gmail.com (L.C.); olivia.gross.amat@free.fr (O.G.-A.)
† Those authors contributed equally to this paper.

Abstract: Second-degree burns result in the loss of the epidermal barrier and could lead to delayed complications during the healing process. Currently, therapeutic options to treat severe burns are limited. Thus, this work aims to evaluate the effect of NaHS, a hydrogen sulfide (H_2S) donor, in poloxamer hydrogel in topical application and the potentiating effect of injected encapsulated adipose-derived stem cells (ASCs) compared to monolayer ASCs using our previous second-degree burn model on human skin explants. Indeed, our model allows testing treatments in conditions similar to a clinical application. The observed benefits of NaHS may include an antioxidant role, which might be beneficial in the case of burns. Concerning ASCs, their interest in wound healing is more than well documented. In order to evaluate the efficiency of our treatments, we analyzed the kinetics of wound closure, keratinocyte proliferation, and dermal remodeling. The effect of NaHS led to a delay in re-epithelialization, with a decrease in the number of proliferating cells and a decrease in the synthesis of procollagen III. On the contrary, intradermal injection of ASCs, encapsulated or not, improves wound healing by accelerating re-epithelialization and collagen I synthesis; however, only encapsulated ASCs accelerate keratinocyte migration and increase the rate of procollagen III and collagen III. In conclusion, NaHS treatment did not improve burn healing. However, the injection of ASCs stimulated wound healing, which is encouraging for their therapeutical use in burn treatment.

Keywords: burn; human skin; ex vivo; wound healing; H_2S treatment; ASC treatment; encapsulation

Citation: Capin, L.; Gross-Amat, O.; Calteau, M.; Rovere, M.-R.; Salmon, D.; Auxenfans, C. NaHS-Hydrogel and Encapsulated Adipose-Derived Stem Cell Evaluation on an Ex Vivo Second-Degree Burn Model. *Eur. Burn J.* **2021**, *2*, 9–30. https://doi.org/10.3390/ebj2010002

Academic Editor: Naiem Moiemen

Received: 6 January 2021
Accepted: 15 February 2021
Published: 19 February 2021

1. Introduction

A second-degree or partial-thickness burn penetrates into but not through the dermis. This kind of wound is, therefore, not harmless, as the epidermal barrier is lost, while the wound could form a blister or, if uncovered, weeps interstitial fluid. Since the dermal plexus of vessels and nerves is intact, the wound blanches with pressure and the pain is severe [1]. Moreover, delayed complications may occur during the healing process requiring then the use of surgical treatments [2,3]. Currently, for second-degree burns, reference treatment consists of the topical application of 1% silver sulfadiazine which does not improve re-epithelialization or the quality of the scar [4,5]. The management of extensive and deep burns, such as epidermal sheets, is costly and requires qualified personnel [6]. It is, thus, essential to find new treatments for second-degree burns and test them on a reliable and standardized model as close as possible to physiological conditions to get relevant results and to limit animal studies. Because the human skin and human wound healing process show specificities, the model used must be reproducible and humanly applicable to test

the effectiveness of treatments. This is why the use of an ex vivo model of human skin seems to be a relevant choice as it enables conditions similar to physiological conditions with all the structures and different cell types resident in human skin in vivo. Although the ex vivo model offers many advantages for the study of burn actives, few studies have established burn models on human skin [7–11]. The interest of our study was to evaluate new potential therapies in a second-degree burn context with our previously developed ex vivo model [12]. Indeed, studies using an ex vivo burn model have not been followed by a test to target a treatment or a wound healing signaling pathway. Only one of these studies investigated the impact of an active ingredient [11]; however, as in many ex vivo skin repair studies, the treatment was added to the culture medium [13,14]. Instead, our study focused on the evaluation of two treatments administered via two different routes: a topical application and an intradermal injection.

We decided to test NaHS, which is a fast hydrogen sulfide (H_2S) donor, and encapsulated ASCs (EN) as a burn treatment on our second-degree burn model. H_2S is found in particular in some sulfur thermal baths. Cures in these thermal waters have been used ancestrally in the treatment of inflammatory dermatological pathologies such as psoriasis, atopic dermatitis, and chronic wounds [15–18]. Although the molecular and cellular effects of H_2S have not yet been defined, the observed benefits may include an antioxidant role, which may also be beneficial in the case of burns that result in increased ROS with a risk of oxidative stress [19–22]. The antibacterial and antifungal role of H_2S could also help to improve wound healing. [23–26]. Although controversial, some studies indicated an anti-inflammatory effect of H_2S, which could be responsible for the improvement of inflammatory skin pathologies [27–30]. The second target of our study was the injection of ASCs as a burn treatment. Even if the entire mechanism of action is not totally understood, the scientific community agrees on the fact that ASCs have huge potential in wound healing through their regenerative properties. Indeed, due to their plasticity [31] and their secretome [32], ASCs are especially interesting in tissue repair. They could improve angiogenesis [33], and they have immunomodulatory properties [34], as well as antifibrotic [35] and chemoattractant effects [36]. Moreover, their paracrine effect is able to influence cell behavior within a pathological environment [37,38]. In the particular case of burns, ASC treatment could potentially resolve immune system dysfunction, re-epithelialization delay, or the appearance of hypertrophic scar [39]. To potentialize the therapeutic effect of injected ASCs, the strategy with the most potential appeared to us to be microencapsulation. According to our previous results [40], encapsulation presents numerous advantages over the direct injection route. In addition to maintaining good cell survival, encapsulation increases and enriches the ASC secretome and recreates physiological conditions by mimicking the native ASC microenvironment without altering stem-cell properties.

In this study, our objective was to test the effect of a chemical active and a cellular therapy as possible treatments for the improvement of second-degree burns. We evaluated the efficiency of a topical application of NaHS in a poloxamer hydrogel, as well as the potentiating effect of microencapsulation of ASCs in a dermal injection compared to monolayer ASCs. In this context, the use of monolayer ASCs (MO) is a way to evaluate the potential benefits of encapsulation.

2. Materials and Methods

2.1. Ethical Statement

Skin samples were anonymized, and informed consent was obtained in accordance with the ethical guidelines from Lyon University Hospital (Hospices Civils de Lyon) and the principles of the Declaration of Helsinki. All the samples used in this study belong to a collection of human skin samples declared to the French research ministry (Declaration no. DC-2008-162 delivered to the Bank of Tissues and Cells of the Hospices Civils de Lyon).

2.2. Skin Explant: Burn Procedure and Culture

All skin explants were obtained from residual tissues generated during elective abdominoplasties. Burn management was carried out as previously explained [12]. Briefly, the skin explant was degreased, quickly rinsed with 70% ethanol, and washed in phosphate buffer solution (PBS) for 30 min. After obtaining a skin with a hexagonal shape of 2.5 cm on each side, it was sutured at each corner on a metal grid in order to produce mechanical tension. Burns were carried out with a 10 s application of a metal rod immersed in water heated to 100 °C. Several burns can be performed on an explant in order to compare different treatments. Debridement of the burn was performed 12 h post burn using a sterile compress.

A culture medium composed of DMEM (Dulbecco's Modified Eagle Medium) supplemented with 10% FCS (Fetal Calf Serum) and antibiotics (20 mg/mL gentamicin (Phanpharma), 100 IU/mL penicillin (Phanpharma), and 1 mg/mL amphotericin B (Phanpharma)) was added the skin to create an air/liquid interface and replaced every other day.

2.3. NaHS Hydrogel Treatment

A poloxamer hydrogel was used as a vehicle for testing the impact of NaHS on our burn model. The hydrogel generously provided by Dr. Salmon (EA4169 "Fundamental, Clinical and Therapeutic Aspects of Skin Barrier Function", University of Lyon 1, Lyon, France) was composed of 25% p407 and p188 (5:1) poloxamers diluted in PBS 1×. With this composition of poloxamers, the generated hydrogel is liquid at temperatures < 30 °C and acquires the physical features of a gel at temperatures > 30 °C. Since skin explants are cultured at 37 °C, the applied hydrogen was maintained on the site of tested skin area.

For each experiment, a fresh solution of 0.25 M NaHS (Sigma-Aldrich, St Louis, MO, USA) dissolved in PBS was prepared and then added to a poloxamer hydrogel to obtain the working concentration (0.25 mM–0.5 mM). The addition of NaHS to the poloxamer hydrogel did not alter the gel consistency or jellification point of the gel. The addition of NaHS did not change the thermosensitive properties of the poloxamer hydrogel.

The poloxamer hydrogel with or without NaHS was applied immediately after preparation on the burn. The poloxamer hydrogel without NaHS was the negative control. The hydrogel was applied daily to the burn and removed after 6 h on three skin donors.

2.4. Origin, Isolation, and Culture of ASCs

ASCs were obtained from three patients (women aged 43.3 years old (range: 35–56), with a BMI (Body Mass Index) of 22.5 kg/m^2 (range: 22–23.4)), undergoing liposuction of abdominal subcutaneous adipose tissue under general anesthesia in the department of plastic and reconstructive surgery at Lyon university hospital. Liposuction was performed with a PAL® LipoSculptor™ (MicroAire Aesthetics, Charlottesville, VA, USA) using a 3 mm Coleman cannula. The volume of adipose tissue obtained was greater than 500 mL. Surgical residue was collected in line with French regulations, and our activity was declared to the French ministry for research (DC n°2008-162).

The stromal–vascular fraction (SVF) was isolated as previously described [40]. Freshly isolated ASCs were seeded at a density of 40,000 cells/cm^2 (passage 0, P0) in proliferation medium—DMEM Glutamax (Gibco), 10% FCS (HyClone), 10 ng/mL GMP-grade fibroblastic growth factor (FGF-2 GMP-grade, Miltenyi Biotec, Bergisch Gladbach, Germany), 100 U/mL penicillin (Panpharma, Fougères, France), 100 µg/mL gentamicin (Panpharma), and 5 µg/mL fungizone (Panpharma)—at 37 °C, under humidified 5% CO_2. The medium was replaced after cells adhered for 1 h, and it was subsequently replaced three times per week. Sub-confluent cell layers (90–95%) were detached using trypsin-EDTA (Ethylenediaminetetraacetic) (Gibco, Thermo Fisher Scientific, Waltham, MA, USA), centrifuged, resuspended in complete medium at 4000 cells/cm^2, and amplified until the number of cells was sufficient for encapsulation.

ASCs were characterized using our previously published protocol [40]. The ASC donors (17,149, 18,019, and 18,020) in this present paper were the same donors as our previously pub-

lished studies [40]. Briefly, the viability was assessed with trypan blue, and metabolic activity was assessed by the MTT (3-(4,5-dimethylthiazol-2-yl)-2,5-diphenyltetrazolium bromide) test. We evaluated the proliferation rate with population doubling and doubling time; to evaluate the differentiation, potential cells were differentiated in the three stipulated lineages by the International Society for Cell-Based Therapy: adipocytes, osteocytes, and chondrocytes. The clonogenical capacity was assessed as colony-forming units. Then, the CD (Class Differentiation) marker expression profiles were assessed by flow cytometry. All the results from these experiments are available in our previous study [40].

2.5. Encapsulation of ASCs in Alginate

ASCs were encapsulated and characterized (differentiation potential, CD markers) as previously explained [40] to obtained microparticles of calcium alginate around 500 µm in diameter. Briefly, sodium alginate (Buchi, France) was dissolved in an aqueous 4% (*w*/*v*) glucose solution to produce sodium alginate solution at 2%. ASCs from each donor were dispersed in 20 mL of this 2% alginate solution, at 4×10^6 cells/mL. Then, cells were encapsulated using the prilling vibration technique using the B-390 Encapsulator (Buchi, France) fitted with a 150 µm nozzle. The droplets of sodium alginate containing encapsulated cells then encountered the aqueous jellification solution, containing 76 mM calcium chloride (Calbiochem, France), 85 mM glucose (Macopharma, France), and 6 mM HEPES (4-(2-hydroxyethyl)-1-piperazineethanesulfonic acid) (Sigma Aldrich, St. Louis, MO, USA) at physiological pH and osmolarity, where the alginate microparticles were formed. Microparticles were rinsed with lactated Ringer's solution (Macopharma, France) and stored in ASC culture medium.

The cell viability before encapsulation was around 97%, whereas it was over 70% after encapsulation for a 16 day period.

2.6. ASC Treatment

Encapsulated (EN) and monolayer (MO) ASCs were used for assessing their impact on wound healing on our burn model. The day after the burn, burnt epidermis was removed and ASCs were intradermally injected at a rate of 400 µL per burn area, corresponding approximately to 350,000 monolayer cells and 175,000 encapsulated cells on six skin donors. We used the cells (encapsulated or not) alone, never with the poloxamer gel which was dedicated to NaHS experiment.

To determine a suitable cell concentration for EN-ASC, after we rinsed the microparticles with Ringer lactate, we took 10 µL of microparticles; after dissolving the alginate with sodium citrate, we counted the cells. We repeated this operation 20 times and the obtained number of cells led to us determining that 400 µL of microparticles corresponded to 175,000 cells. For MO-ASC, the number of cells injected was around 350,000 cells corresponding to a 400 µL volume of cells in Ringer solution. We injected the cells (encapsulated or not) through a 21 G needle (inner diameter (i.d.) 0.80 mm).

2.7. Histological and Immunohistological Analysis of Skin Explants Treated with NaHS and ASCs

The skin explants were harvested and analyzed as explained previously, on days 0, 1, 3, 5, 6, 7, 8, 9, 10, and 14 for NaHS treatment and days 5, 10, and 15 for ASCs treatment [12]. Briefly, the lesioned area was excised and cut into two pieces which were either embedded in OCT (Optimal Cutting temperature) compound and stored at −20 °C until use or immediately fixed with 4% formaldehyde before being embedded in paraffin.

For histological analysis, paraffin-embedded formalin-fixed samples (5 µm), after dewaxing and rehydration, were stained with hematoxylin phloxine saffron (HPS staining: cell nuclei were stained blue with hematoxylin, the cytoplasm was stained pink with phloxine, and the extracellular matrix of connective tissue was stained orange/yellow with saffron). For immunohistochemistry, sections were incubated with HLA (Human Leukocyte Antigen)-R/DP/DQ/DX primary antibody (dilution 1:1500, clone CR3/43, sc-53302, Santa Cruz Biotechnology). For immunofluorescence, slides were incubated

overnight at 4 °C with the following primary antibodies: Ki67 (dilution 1:50, clone MIB-1, GA626, DakoCytomation, Glostrup, Denmark), procollagen III (dilution 1:500, clone M-58, Merck, Darmstadt, Germany), α-SMA (α-Smooth Muscle Actin) (dilution 1:200, NCL-L-SMA, Novocastra Laboratories), collagen I (dilution 1:500, Novocastra Laboratories), and collagen III (dilution 1:250, Novocastra Laboratories). Nuclei were colored by a blue Hoechst staining (1:1000, Thermo Fisher Scientific, Waltham, MA, USA).

Image acquisition was performed using a slide scanner (Axioscan Zeiss) in order to enable a global view of the whole burnt area and of adjacent non-lesioned tissues.

2.8. Image Analysis

Image processing and analysis were performed using the Image J software (Research Service Branch, US National Institute of Health, United States). Ki67-positive epidermal cells were counted and expressed as a percentage relative to the total number of nuclei in the epidermal area analyzed. For α-SMA, procollagen III, collagen I, collagen III, and HLA, the surfaces covered by staining were measured and expressed as a percentage relative to the total dermal area analyzed. When needed, measurements were performed at both edges of the burnt area, as well as at the center of the lesioned area. To perform our measures, we used a program within Image J software where we selected a threshold (the same for each image but specific to each staining) from which the area could be considered as stained compared to negative control.

For epidermis thickness, an average of four measurements were performed at both edges of the burnt area, as well as at the center of the lesioned area. The measures were performed at the same place on all the images and the images were treated anonymously with only their sample number.

2.9. Statistical Analysis

For all data, GraphPad Prism 4 software (GraphPad Software Inc., La Jolla, CA, USA) was used to determine statistical significance with the paired *t*-test; statistically significant differences are indicated by asterisks as follows: * $p < 0.05$, ** $p < 0.01$.

3. Results

3.1. Impact of NaHS and Encapsulated ASCs on Epidermis on Second-Degree Ex Vivo Burn Model

To investigate the impact of NaHS and encapsulated ASCs on the second-degree ex vivo burn model, histological analysis and Ki67 immunostaining were performed.

NaHS was tested in poloxamer hydrogel at 0.25 mM and 0.5 mM on lesioned skin explant samples obtained from three distinct donors. The negative control was a topical application with poloxamer hydrogel without NaHS. In order to assess the impact of NaHS treatment on wound closure kinetics. The extent of re-epithelialization was assessed on days 0, 1, 3, 5, 6, 7, 8, 9, 10, and 14 post burn by HPS, as described previously [12]. Days of interest were subsequently analyzed by immunostaining. Daily topical applications of such a poloxamer hydrogen were performed on areas of lesioned skin explants in our model of experimental second-degree burn injury with or without NaHS (0.25 or 0.5 mM). On day 10 of the culture, we observed a similar re-epithelialization for the different conditions with or without NaHS (Figure 1) with an advancement of the epidermal tongue allowing closure by the wound edges. On the other hand, on day 14, we observed that wounds treated were not completely re-epithelialized at 0.25 mM NaHS (Figure 1b) and blocked at 0.5 mM (Figure 1c), compared to those treated with hydrogel alone (Figure 1a). In addition, at 0.25 mM NaHS, the epidermal advance contained fewer (1–2) layers of keratinocyte cells (Figure S1, Supplementary Materials) compared to the 4–5 layers for control (Figure S1, Supplementary Materials). Treatment at 0.5 mM NaHS had a more detrimental effect on the keratinocytes; on day 14, there was a regression of epidermal tongue advancement, with only one layer of keratinocytes remaining, and the wound remained completely open (Figure 1c and Figure S1, Supplementary Materials). NaHS then appeared to have a dose-dependent effect, resulting in delayed re-epithelialization.

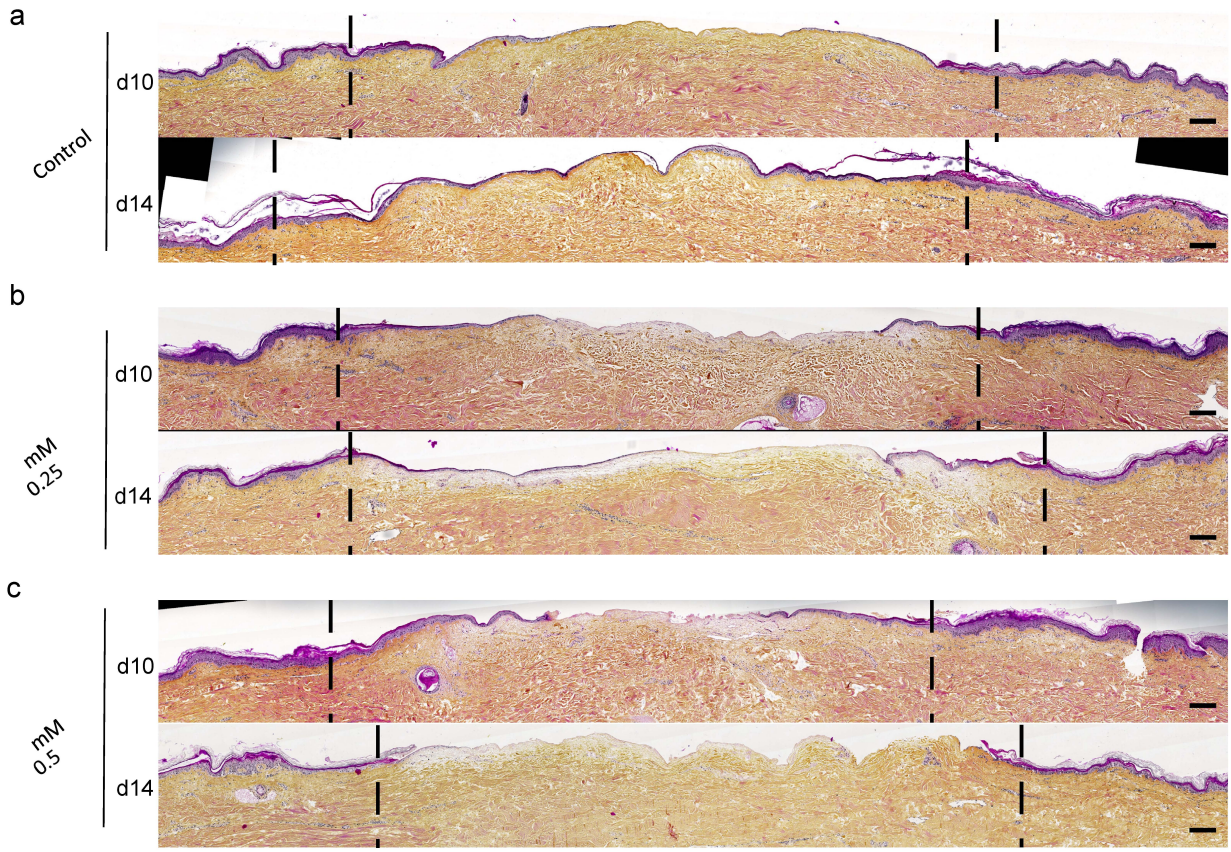

Figure 1. Histological analysis of second-degree ex vivo burn model after treatment with poloxamer hydrogel containing NaHS (0.25 mM–0.5 mM). The impact of NaHS on burn re-epithelialization was observed by hematoxylin phloxine saffron (HPS) staining at different times of culture (day 10 and day 14): (**a**) poloxamer hydrogel alone (control) and (**b**) 0.25 mM or (**c**) 0.5 mM NaHS–poloxamer hydrogel. The control burn treated with poloxamer hydrogel alone was completely re-epithelized on day 14 (**a**), whereas it is not complete for lesions treated with NaHS (**b**,**c**). On day 14, we observed that a 0.25 mM NaHS treatment decreased the re-epithelialization of the epidermis (**b**). A 0.5 mM NaHS treatment resulted in a non-re-epithelialized wound. Moreover, the epidermal tongue observed on day 10 was no longer visible on day 14 (**c**). Dashed lines in black delineate the burnt area. Experiments were performed on skin explants derived from three donors. Scale bar: 100 µm.

We previously observed that NaHS leads to a decrease in epidermal stem cell proliferation [41]. We, thus, verified by immunostaining the Ki67+ proliferating cells relative to the total number of epidermal cells whether the NaHS at 0.25 mM or 0.5 mM in hydrogel poloxamer induced a delay in re-epithelialization compared with hydrogel poloxamer alone. At the wound edges on day 5, we observed no significant difference in the rate of proliferating cells (Figure 2d). On the other hand, on day 8, we observed a higher rate of proliferating cells for control (48%) compared to NaHS-treated lesions (29% at 0.25 mM and 36% at 0.5 mM). This difference in Ki67+ cells at the wound edge was no longer present on day 14 even though re-epithelialization was incomplete with NaHS treatment. Looking at proliferating cells in the center of the burn on day 14, the percentage of Ki67+ cells was similar to the control for the condition treated at 0.25 mM NaHS (Figure 2e). However, when immunostaining was observed (Figure 2a,b), fewer Ki67+ cells were observed in the center of the burn when treated with 0.25 mM (Figure 2b) than for the control condition (Figure 2a). The percentages of Ki67 are similar because the number of Ki67+ cells is related to the total number of cells in the epidermis; however, as mentioned above, the control contained more layers, i.e., more keratinocytes. Therefore, the number of proliferating cells remained higher for the control condition although it was more difficult to compare to conditions with NaHS.

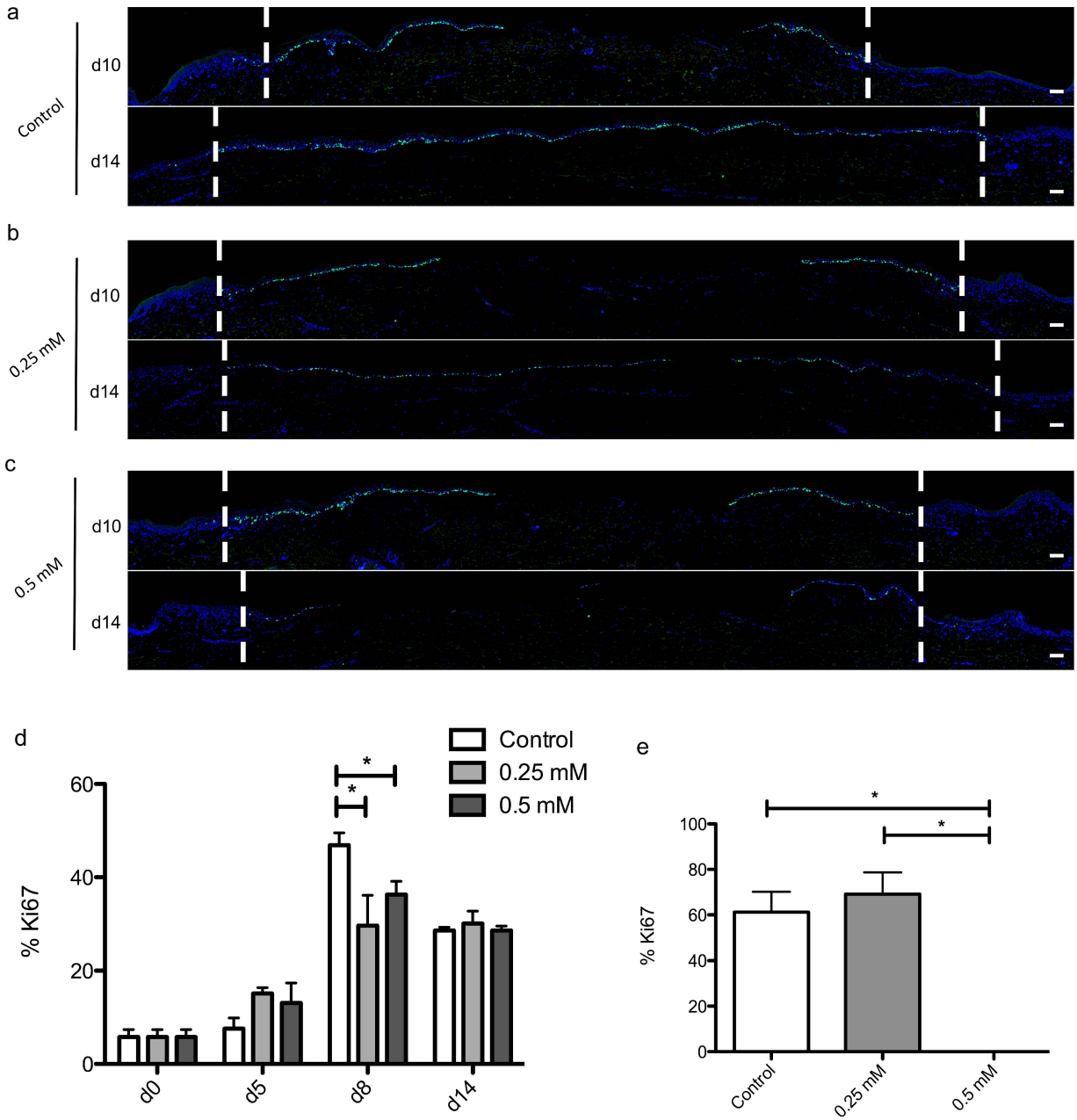

Figure 2. Second-degree ex vivo burn model after treatment with poloxamer hydrogel containing NaHS (0.25 mM–0.5 mM) analyzed by Ki67 immunostaining. Immunostaining of Ki67 was performed on a second-degree burn model harvested at different time points post burn (days 5, 8, 10, and 14): (**a**) poloxamer hydrogel alone (control) and (**b**) 0.25 mM or (**c**) 0.5 mM NaHS–poloxamer hydrogel. Expression of Ki67 is shown in green color and cell nuclei are shown in blue color The proliferation index of keratinocytes (ratio of proliferating Ki67+ cells relative to the total number of epidermal cells) was measured in human skin explants harvested at different time points of the culture. On day 8, at the lesion edges, a decrease in proliferation was observed for lesions treated with NaHS–poloxamer hydrogel (48% in hydrogel-treated lesions vs. 29% and 36% in lesions treated with 0.25 mM and 0.5 mM NaHS hydrogel, respectively). On day 14, the proliferation index was similar in the different conditions with or without NaHS only at the lesion edges because, in the center of the burn (**e**), there were no cells on the lesion treated with the hydrogel containing 0.5 mM NaHS. For each donor and for each time point, measurements were carried out at the edges (**d**) or at the center (**e**) of the lesion and expressed as mean values. Dashed lines in white (**a**–**c**) delineate the burnt area. Experiments were performed on skin explants derived from three donors. Statistical significance was assessed with the paired *t*-test. * $p < 0.05$. Scale bar: 100 µm.

Although a blockage of the re-epithelialization was observed with the treatment at 0.5 mM NaHS after 14 days, a large proportion of proliferating cells were observed on day 10. At the border on day 14, although progress was significantly reduced, proliferating cells were still present. NaHS appeared to slow down the proliferation without inhibiting it completely.

Encapsulated ASCs were injected on a second-degree ex vivo burn model from six distinct donors. (Figure 3a). Monolayer ASCs (MO) or encapsulated ASCs (EN) were injected in the dermis of distinct burnt areas. No cells were injected in the negative control (NC) in order to assess the impact of ASC treatment on wound closure kinetics. Five days post burn, the entire burn area was visible in the three conditions with few signs of re-epithelialization on treated skins. This observation was confirmed by statistical analysis, as shown in Figure 3b. Interestingly, on day 10 (Figure 3a), the epidermis of explants treated with MO-ASCs and EN-ASCs was almost fully restored, whereas the re-epithelialization barely began in the negative control. However, according to epidermal thickness analysis, the only significant difference was between skin treated with MO and EN ASCs. Epidermis from explants treated with MO-ASCs appeared thicker than that obtained after EN-ASC treatment. However, on day 15, a complete re-epithelialization was observed in all conditions. In explants treated with MO-ASCs, a thickening of the epidermis was observed on images at the center of the wound, while the new epidermis obtained with EN-ASCs treatment was more homogeneous. Nevertheless, ASC injection and, particularly, encapsulated ASC injection damaged the dermis. In MO and EN conditions, holes were observed as evidence of the dermis deterioration. According to these results, ASC treatment appeared to accelerate the wound closure and improve re-epithelialization in spite of dermis deterioration.

In order to assess the impact of ASC treatment on keratinocyte proliferation, immunostainings of Ki67 were performed on human skin explants on days 5, 10, and 15 after the burn in the three conditions: explant treated with monolayer ASCs (MO), explant treated with encapsulated ASC (EN), and explant not treated, i.e., negative control (NC) (Figure 4). In the negative control on day 5, keratinocytes started to proliferate on the edges of the burn, whereas, in explants treated with MO-ASCs and EN-ASCs, keratinocytes already reached the center of the burn (Figure 4a). However, this difference in proliferation on day 5 between the explants treated and negative control was not found in the statistical analysis, as shown in Figure 4b. Indeed, the analysis of the proliferation rate on the edges of the burn, defined as the ratio of proliferating Ki67+ cells relative to the total number of epidermal cells, only revealed a difference of 8.2% on day 10 between MO and EN conditions. Thus, on day 10 post burn, there were fewer keratinocytes proliferating on the edges of the burn in the EN condition than in the MO condition. Keratinocytes in the EN condition migrated to the center of the burn earlier than in the MO condition but this difference was not confirmed when compared with the negative control. Nevertheless, while differences in keratinocyte proliferation on the edges of the burn were not clearly demonstrated between the three conditions, statistical analysis showed a significative difference in keratinocyte proliferation at the center of the burn (Figure 4c). Indeed, on day 15 post burn, there were 7.9% more keratinocytes proliferating at the center of the wound in the EN condition than in the negative control. The encapsulated ASC treatment accelerated the proliferation process by improving keratinocyte migration to the center of the burn.

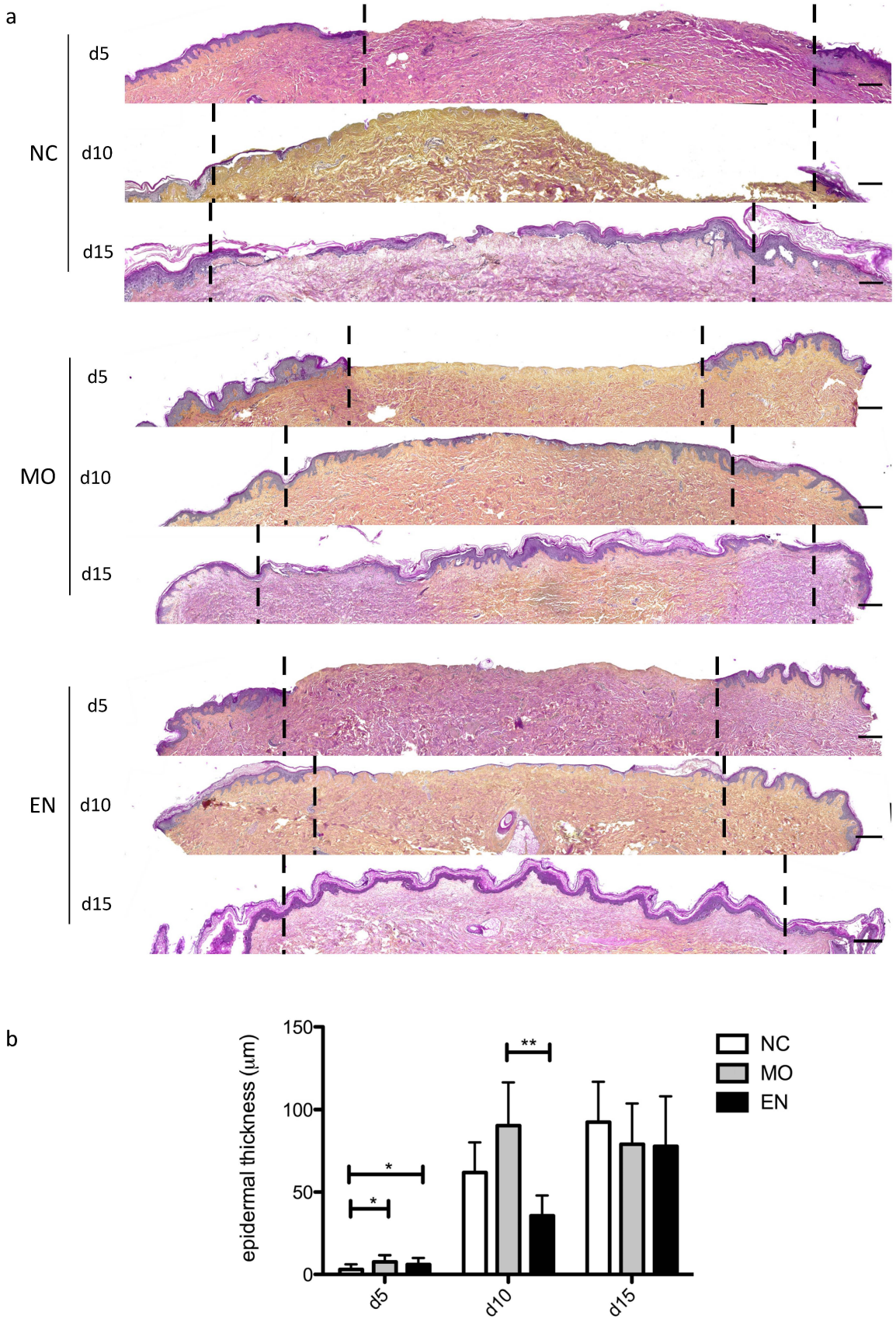

Figure 3. Histological analysis of second-degree ex vivo burn model after treatment with ASCs. (**a**) Encapsulated (EN) and

monolayer (MO) ASCs were intradermally injected. In the negative control (NC), no cells were injected. The impact of ASC treatment on burn re-epithelialization was observed by HPS staining at different times of the culture (days 5, 10, and 15). Explants treated with monolayer ASCs (MO) and encapsulated ASCs (EN) were already re-epithelialized on day 10, whereas re-epithelialization of the control burn (NC, not treated) just started at this time point. Dashed lines in black delineate the burnt area. (**b**) Epidermal thickness was measured using Image J® at the center of the burn at three time points (days 5, 10, and 15) on images of HPS staining. On day 5, explants treated with ASCs already started their re-epithelialization, and the epidermis obtained after MO-ASC treatment appeared thicker than that obtained after EN-ASC treatment on day 10. For each donor and for each time point, measurements were carried out at the center of the lesion and expressed as mean values. Experiments were performed on skin explants derived from six donors. Statistical significance was assessed with the paired *t*-test. * $p < 0.05$, ** $p < 0.01$. Scale bar: 100 µm.

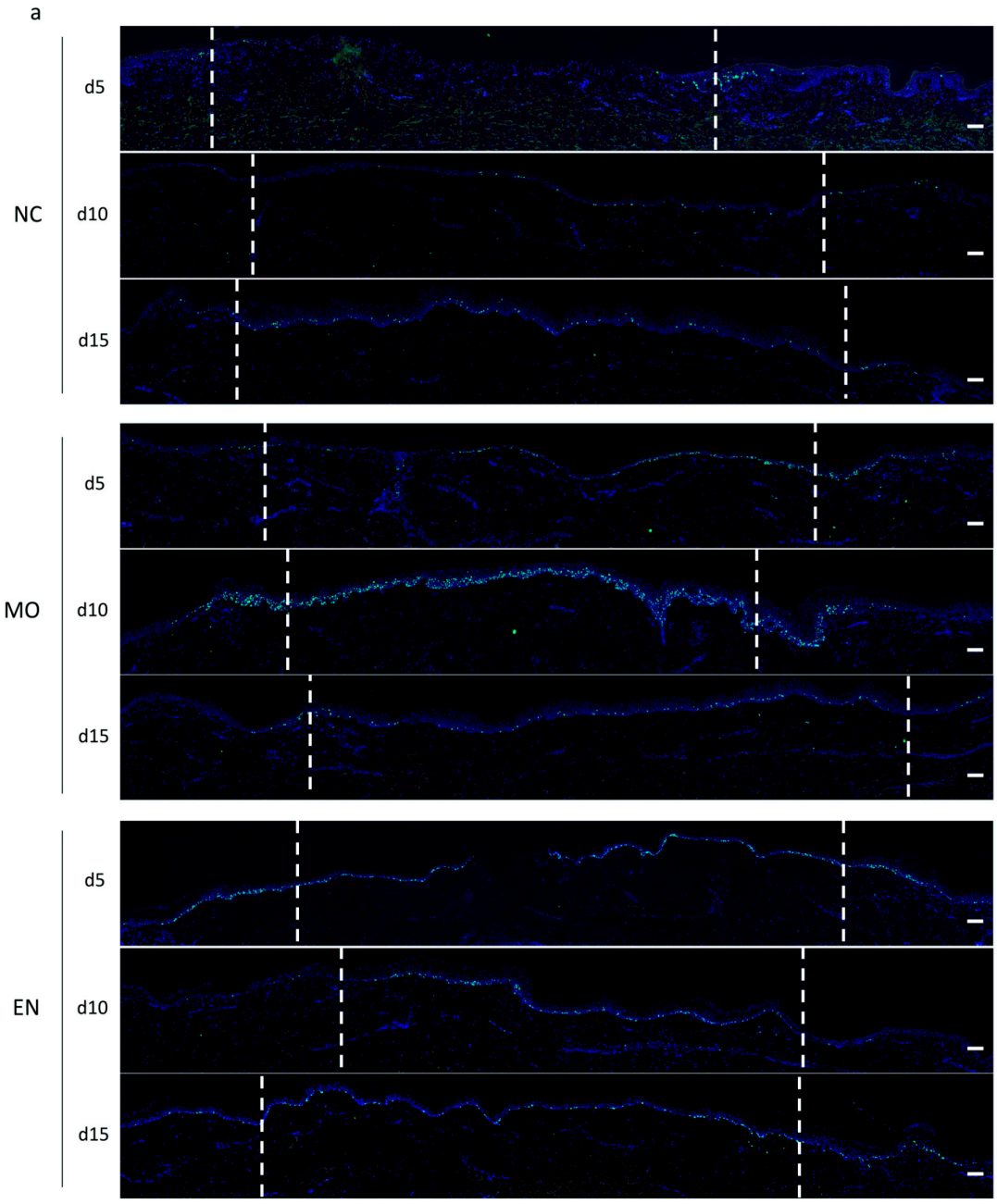

Figure 4. *Cont.*

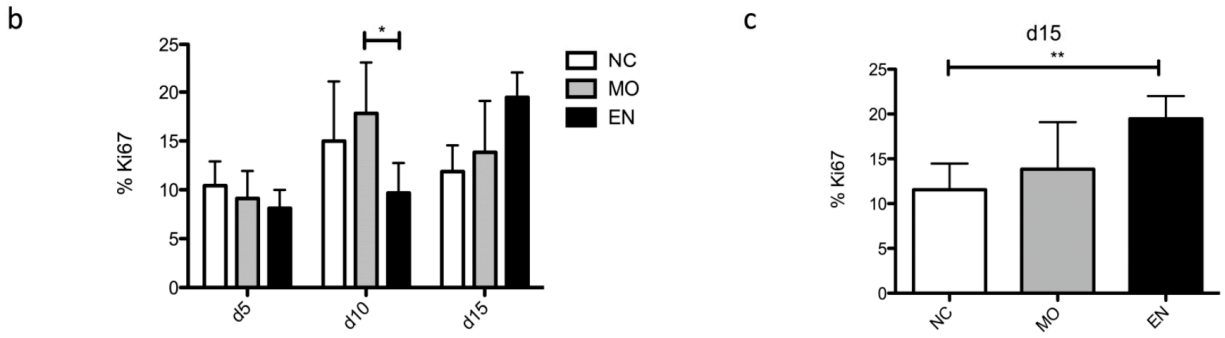

Figure 4. Second-degree ex vivo burn model after treatment with ASCs analyzed by Ki67 immunostaining. (**a**) Encapsulated (EN) and monolayer (MO) ASCs were intradermally injected. In the negative control (NC), no cells were injected. Expression of Ki67 at 5, 10, and 15 days is shown in green color and cell nuclei are shown in blue color. Dashed lines in white delineate the burnt area. (**b**) The proliferation index of keratinocytes (ratio of proliferating Ki67+ cells relative to the total number of epidermal cells) was measured at the edges of human skin explants harvested at different time points of the culture. On day 10, at the lesion edges, a decrease in proliferation was observed for lesions treated with EN ASCs compared to MO ASCs, but not to NC. (**c**) The proliferation index of keratinocytes (ratio of proliferating Ki67+ cells relative to the total number of epidermal cells) was measured in human skin explants harvested after 15 days of the culture on the center of the burn. An increase in proliferation was observed for explants treated with EN ASCs compared to negative control. Experiments were performed on skin explants derived from six donors. Statistical significance was assessed with the paired *t*-test. * $p < 0.05$, ** $p < 0.01$. Scale bar: 100 μm.

We, therefore, observed opposite effects of the two tested treatments with deleterious effects of NaHS and stimulating effects of encapsulated ASCs on re-epithelialization and keratinocyte proliferation.

3.2. Impact of NaHS and Encapsulated ASCs on Dermis in Second-Degree Ex Vivo Burn Model

We also investigated the impact of NaHS in dermal proteins. An analysis of different proteins was performed (αSMA, collagen I, collagen III, and procollagen III) on three donors. Although we were able to identify that, following the burn, in this ex vivo model, we did not observe any evolution in the staining for αSMA, collagen I, and collagen III [12], it was interesting to see if the NaHS could nevertheless modify these proteins. However, we did not observe any differences between the conditions independent of the culture day for the proteins αSMA (Figure S2, Supplementary Materials), collagen I (Figure S3, Supplementary Materials), and collagen III (Figure S4, Supplementary Materials). On the other hand, we observed a decrease in the intensity of procollagen III staining, starting from day 8, similar to the control (Figure 5). In the control condition, this decrease in procollagen occurred on day 10 and returned to a basal level on day 14 (Figure 5a). For wounds treated with NaHS, this decrease in procollagen III intensity was still significant on day 10, as well as on day 14 (Figure 5b,c). On day 14, the area of decrease in intensity of procollagen III was more difficult to delineate, although a difference can be observed when compared with the healthy (border) areas; therefore, the synthesis of procollagen III could be partly achieved although the epidermis was not re-formed.

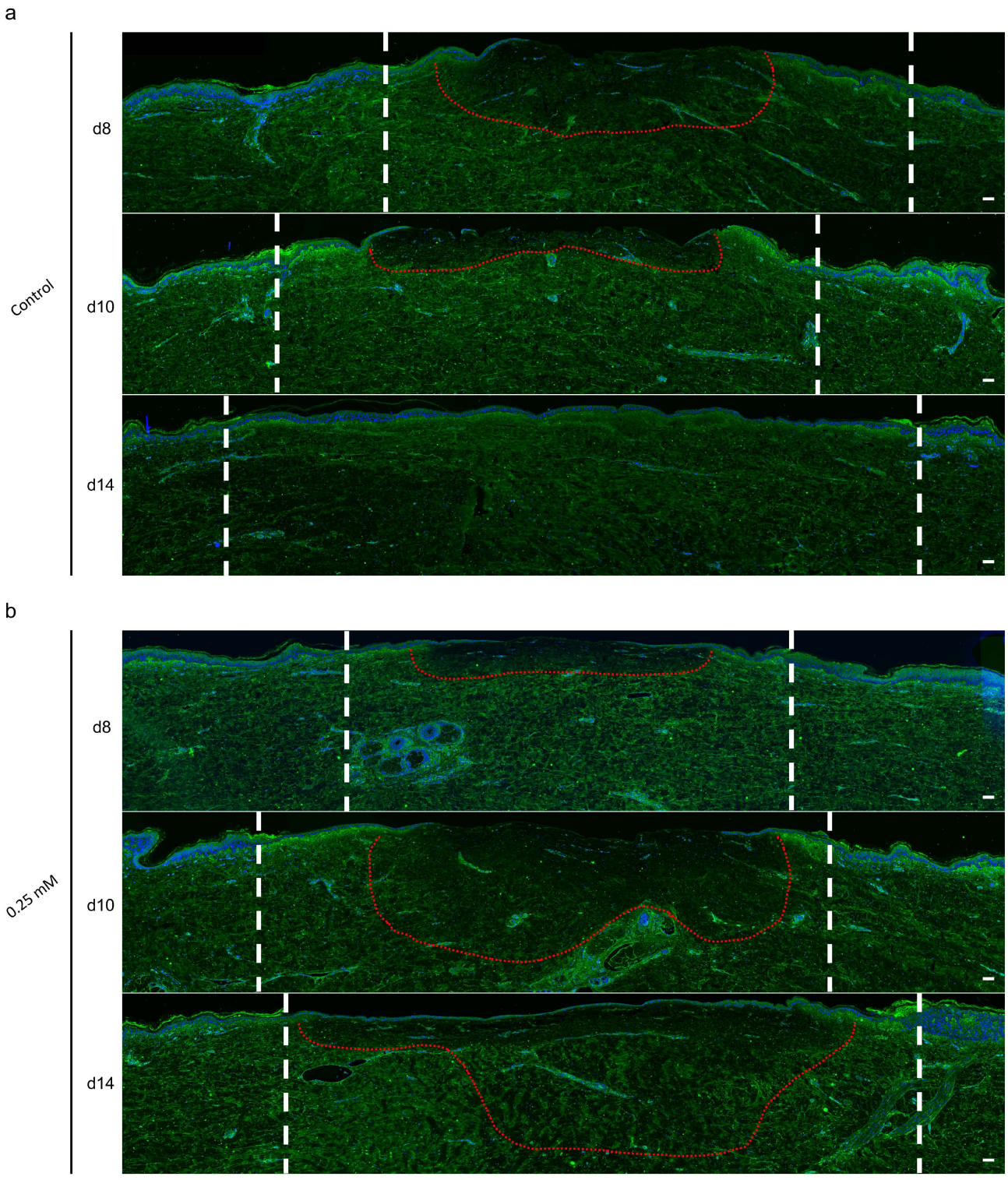

Figure 5. *Cont.*

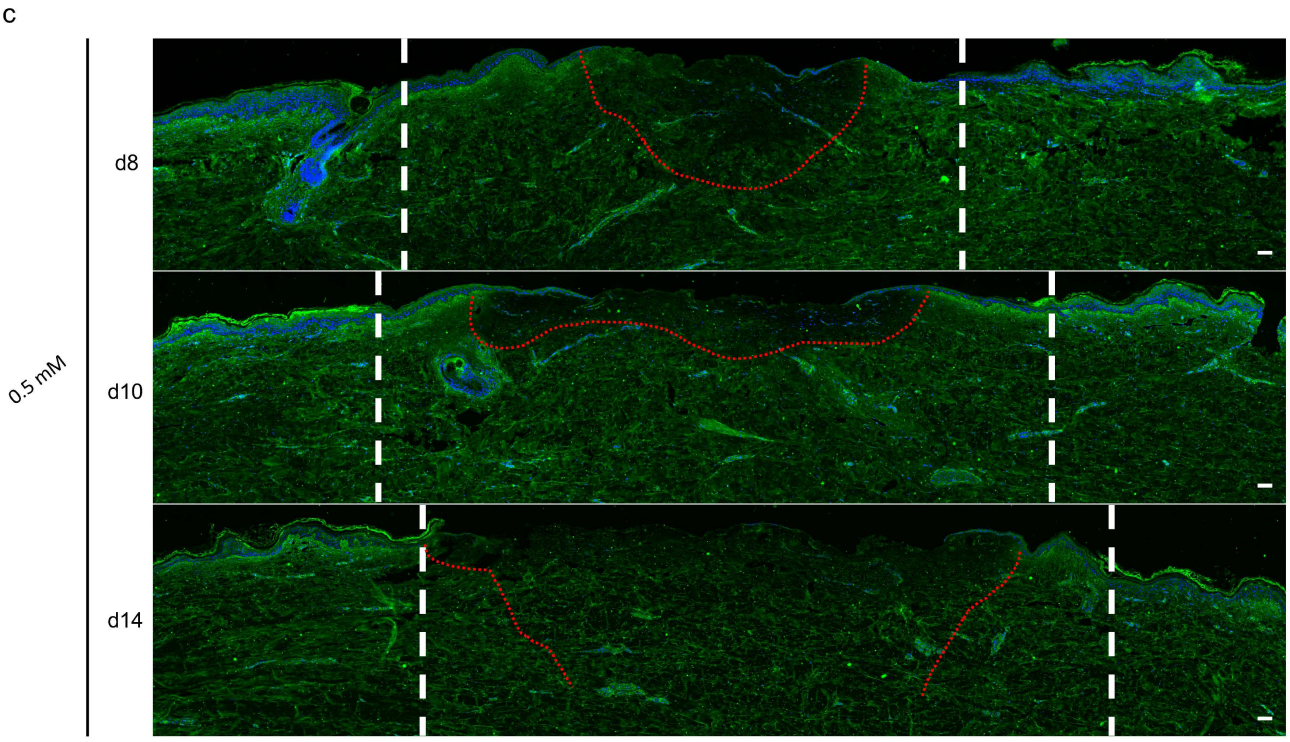

Figure 5. Second-degree ex vivo burn model after treatment with poloxamer hydrogel containing NaHS (0.25 mM–0.5 mM) analyzed by procollagen III. Immunostaining of procollagen III was performed on the second-degree burn model harvested at different time points post burn (days 8, 10, and 14): (**a**) poloxamer hydrogel alone (control) and (**b**) 0.25 mM or (**c**) 0.5 mM NaHS–poloxamer hydrogel. A decrease in intensity of procollagen III staining (area delimited by a red dotted line) was observed on day 8 and still present on day 10 until it returned to baseline levels on day 14. Expression of procollagen III is shown in green color and cell nuclei are shown in blue color. (**b**,**c**) For the NaHS–poloxamer hydrogel treatment, at both tested concentrations, a decrease in procollagen III intensity staining was also observed on day 8; however, it was still present and more expanded on day 10 and day 14. Experiments were performed on skin explants derived from three donors. White dashed lines delineate the burnt area. Scale bar: 100 µm.

Having identified that NaHS stimulates IL-8 (interleukin 8) secretion by keratinocytes in vitro [41], we sought to verify whether NaHS could then stimulate the recruitment of immune cells at the wound site. We then stained wounds treated or not treated with NaHS on different days of the culture with an HLA staining that marks cells with Complex MHC (Major Histocompatibility) class II (macrophages, monocytes, dendritic cells). We observed a slight increase in wound edge staining on day 8 for the NaHS-treated conditions (Figure S5b,c, Supplementary Materials) compared to the control condition (Figure S5a, Supplementary Materials). This increase was not maintained on day 14.

NaHS had a dose-dependent impact, resulting in a delay until wound re-epithelialization was blocked after a second-degree burn, as well as a delay in procollagen III synthesis.

To investigate the impact of ASCs on dermal protein, an analysis of αSMA, procollagen III, collagen III, and collagen I was performed on human explants. Although no differences between conditions independent of the culture day could be observed for αSMA (Figure S6, Supplementary Materials), some differences were observed for collagen synthesis. Indeed, in the negative control (NC), a decrease in the intensity of procollagen III staining was observed in the burn area on days 5 and 10, and this phenomenon was attenuated on day 15 (Figure 6a). However, in explants treated with MO-ASCs (MO), this decrease was not as clearly visible at any time point, although a difference could be observed when compared with the healthy border on days 5 and 10. For the explants treated with EN-ASCs (EN), this decrease in intensity was quite obvious on day 5 but more difficult to delineate on days 10 and 15. Moreover, this difference in procollagen III synthesis was

confirmed by the statistical analysis, as shown in Figure 6b, whereby explants treated with EN-ASCs expressed 6% more procollagen III than the negative control. Thus, ASC treatment (especially EN-ASC treatment) plays a role in procollagen III dermal synthesis.

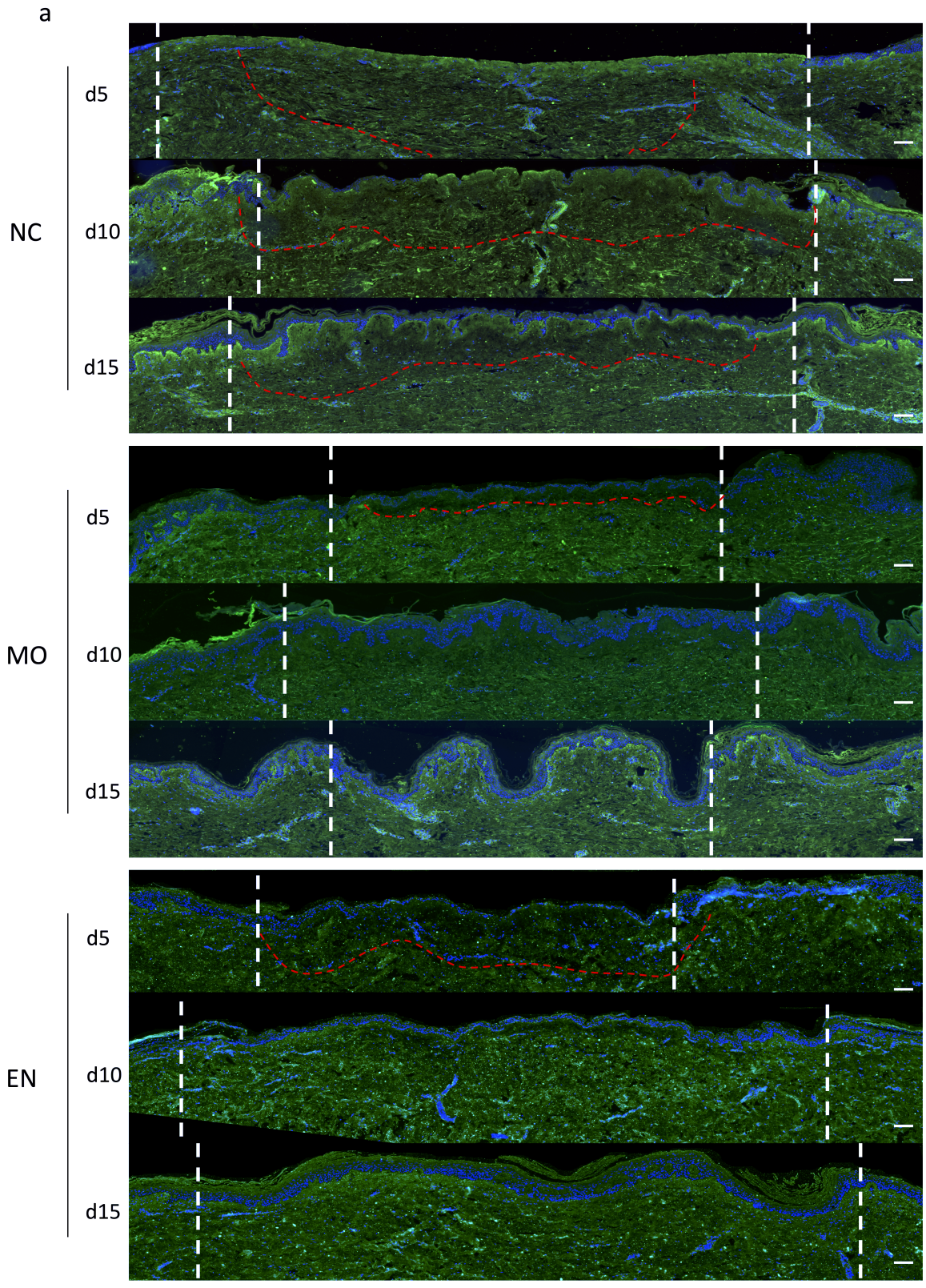

Figure 6. *Cont.*

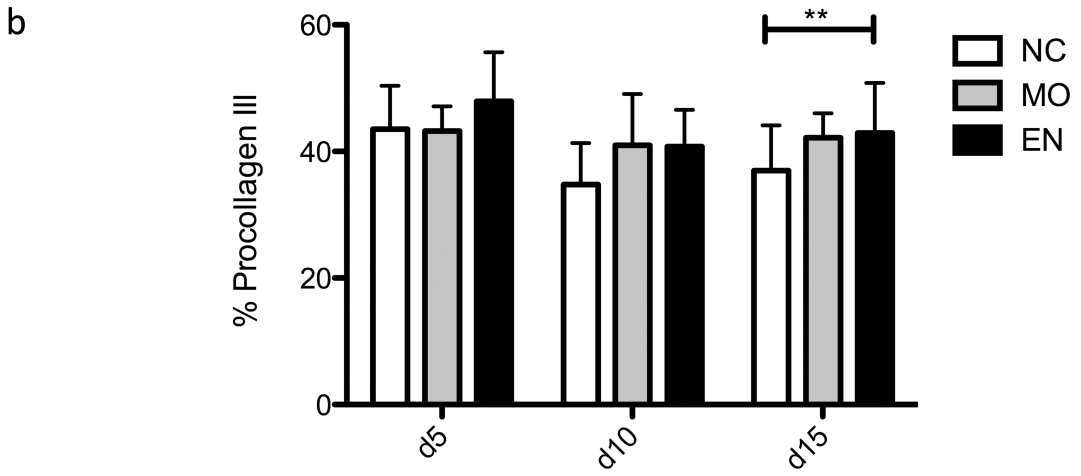

Figure 6. Second-degree ex vivo burn model after treatment with ASCs from six donors analyzed by procollagen III. Immunostaining of procollagen III was performed on ASC-treated second-degree burn model harvested at different time points post burn (days 5, 10, and 15). Encapsulated (EN) and monolayer (MO) ASCs were intradermally injected. In the negative control (NC), no cells were injected. Expression of procollagen III is shown in green color and cell nuclei are shown in blue color. (**a**) A decrease in intensity of procollagen III staining (area delimited by a red dotted line) was observed on day 5 and still present on days 10 and 15 in the negative control. However, for explants treated with monolayer ASCs (MO), this intensity difference was not clearly visible on day 5 and was absent on days 10 and 15. In the explant treated with EN-ASCs, a decrease in intensity of procollagen III staining was observed on day 5 but not on days 10 and 15. White dashed lines delineate the burnt area. (**b**) Procollagen III area was measured at the center of the wound (ratio between procollagen III area and total dermis area). On day 15, burns treated with EN-ASCs appeared to express more procollagen III than negative controls. Experiments were performed on skin explants derived from six donors. Statistical significance was assessed with the paired *t*-test, ** $p < 0.01$. Scale bar: 100 μm.

Collagen III synthesis was also studied in burn explants. Contrary to procollagen III, we could not highlight an intensity difference in collagen III signal between the three conditions. Nevertheless, we observed a slight density difference on day 15 between explants treated with monolayer or encapsulated ASCs and the negative control (Figure S7, Supplementary Materials). Interestingly, this difference was translated by the statistical analysis represented in Figure 7a, which confirmed the difference in collagen III rate between the second-degree burn model treated with encapsulated ASCs (EN) and the negative control (NC). ASC treatment decreased collagen III synthesis in the early phase of the wound healing process by almost 11% (10.9% for MO-ASC treatment and 10.7% for EN-ASCs); then, EN-ASC treatment increased its synthesis by 10.8% on day 15 compared to the negative control.

Then, we analyzed collagen I synthesis at the center of the wound in the three conditions described above at different time points (days 5, 10 and 15). Here again, we could not highlight a difference in the intensity of collagen I signal, and we also did not observe a visual difference in density on day 10 between the treated and non-treated second-degree burn model (Figure S8, Supplementary Materials). However, the rate of collagen I in the dermis appeared more important on day 10 in the explant treated with monolayer and encapsulated ASCs (13.9% and 11.2% more, respectively) than in the negative control (Figure 7b). This finding, coupled with previous outcomes, seems to suggest that ASCs improve the wound healing process by accelerating the kinetics of collagen I appearance.

Intradermal injection of human monolayer or encapsulated ASCs improves wound healing by accelerating re-epithelialization and collagen I synthesis; however, only intradermal injection of human encapsulated ASCs accelerates keratinocyte migration and increases the rate of procollagen III and collagen III in a second-degree burn model.

The two tested treatments showed opposite effects on procollagen III synthesis, which was inhibited by NaHS and stimulated by ASCs. Only ASC treatment has an impact on collagen I and III.

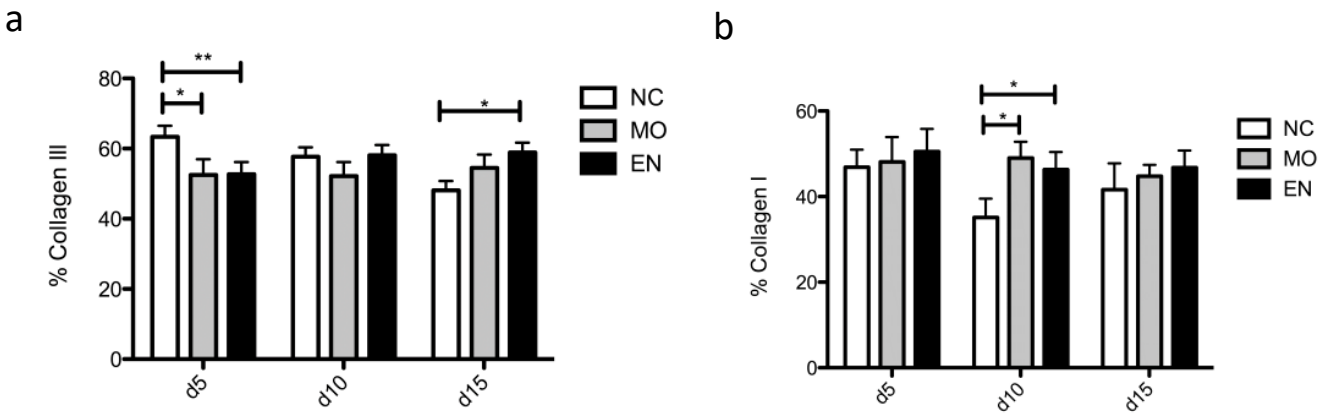

Figure 7. Kinetics of collagen III and I dermal expression in ASC-treated second-degree burn model (**a**). Collagen III area was measured at the center of the wound (ratio between collagen III area and total dermis area). On day 5, it appears that there was more collagen III in the negative control (NC) than in burns treated with monolayer (MO) and encapsulated (EN) ASCs, and this trend was reversed on day 15 with a 10% increase in the collagen III surface in explants treated with EN-ASCs compared to the negative control. (**b**) Collagen I area was measured at the center of the wound (ratio between collagen I area and total dermis area). On day 10, an increase in collagen I surface was observed in ASC-treated second-degree burn model (MO and EN) compared to NC. Results obtained for each condition are representative of six series of experiments performed on skin explants derived from six donors. Statistical significance was assessed with the paired *t*-test. * $p < 0.05$, ** $p < 0.01$.

4. Discussion

We were able to observe the impact of two different target treatments on improving skin healing. It is interesting to note that we encountered results of decreased skin repair with the application of poloxamer hydrogel containing NaHS, whereas a stimulation of healing was observed with the injection of ASCs.

The effect of NaHS led to a delay in re-epithelialization, with a decrease in the number of proliferating cells at 0.5 mM NaHS and a decrease in the synthesis of procollagen III at the burn site. NaHS then caused a delay in procollagen III synthesis, either by acting directly on the fibroblasts of the dermis or by inducing the delay/blockage of re-epithelialization, whereby the keratinocytes did not send, or sent in lesser numbers, the signals enabling procollagen III synthesis.

As mentioned above, the role of H_2S is still poorly understood, and it is associated with both proinflammatory and anti-inflammatory effects [42–48]. However, these results are in line with our findings showing that NaHS leads to a decrease in the proliferation of primary human keratinocytes. In addition, an increase in the secretion of proinflammatory cytokines (IL-8, CXC Motif Chemokine Ligand 2—CXCL2, IL-18, and IL-1β) was observed [41]. This increase could lead to an increase in inflammatory cells in the wound and explains the increase in HLA marker after the addition of NaHS.

Concerning the NaHS impact on keratinocyte proliferation, these results are consistent with our previous results on primary keratinocytes in vitro [41], indicating an inhibitory dose-dependent impact of NaHS on keratinocyte proliferation. However, the impact of 0.5 mM NaHS leading to the regression of keratinocyte advancement could be due to another process of NaHS which remains to be investigated. Furthermore, the procollagen III synthesis delay could be impacted by a delay in proliferation, as well as increased inflammation, at the wound edge.

Although these results do not explain the benefits of sulfurous thermal waters in the treatment of chronic ulcer repair, they may shed some light on their impact on psoriasis. Indeed, patients with psoriasis develop plaques caused by hyperproliferation of keratinocytes [49,50]. H_2S could then improve this symptom by decreasing keratinocyte proliferation, thus improving patients' quality of life. It would then be interesting to develop at least one skin culture model of a psoriasis patient, as has been done for different types of scars (keloid, hypertrophic scar) studied in ex vivo culture after sampling from human patients [51]. Our model did not permit the evaluation of the antimicrobial role of H_2S. Indeed, human skin explants are grown in a sterile environment after being bathed in antibiotics. The beneficial effect of H_2S in wound healing could be mainly due to its antimicrobial action, as in the commonly used cream containing 1% silver sulfadiazine [4,52].

Concerning the ASCs, the aims were to assess their impact on wound healing in a second-degree burn model and evaluate if encapsulation improved this action. Cellular microencapsulation was developed both to reduce premature death of cells following injection and to limit their migratory capacity [53,54]. In this study, adipose stem cells were reproducibly encapsulated as previously described [40], using a prilling vibration method, in microparticles of alginate, a biocompatible and biodegradable polysaccharide [55,56].

According to the literature, ASCs generate real interest in wound healing due to their anti-inflammatory and immunomodulatory effect [57,58], through their secretion which promotes angiogenesis, as well as keratinocyte proliferation and migration [59]. In our study, results obtained after HPS staining support these findings. Indeed, both monolayer (MO) and encapsulated (EN) ASCs improved wound closure kinetics with an acceleration of re-epithelialization. In our second-degree burn model, keratinocytes migrated faster from the edges to the center of the burn in explant treated with encapsulated ASCs than in the negative control. According to the pictures, this action on keratinocyte migration started on day 5 and occurred in MO and EN conditions, but it was not found in the statistical analysis, potentially due to the limited number of donors studied. However, as described in the literature [36,60], ASCs demonstrated their homing property on keratinocytes in our second-degree burn model, which was improved by encapsulation. Five days post burn, the re-epithelialization was extensive in the explants treated with MO and EN ASCs, whereas this was not indicated in the negative control. Moreover, in some donors, re-epithelialization started before day 5 in MO and EN conditions. Another interesting fact is that the epidermis formed in explants treated with MO-ASCs appeared thicker than that obtained with EN-ASCs in the images on days 10 and 15, as well as in statistical analysis. If we admit that encapsulation increases and enriches ASC secretion, as shown in a previous study [40], this could be the reason why the scar obtained with EN-ASCs was of better quality. EN-ASCs would be able to better regulate keratinocyte proliferation and matrix formation. Another hypothesis is that EN-ASCs might have a role in senescence slowdown, which may explain the increase in keratinocyte proliferation on day 15. Indeed, this effect was not observed with MO-ASCs and the negative control. However, we need to further assess the action of encapsulated ASCs on the epidermis, dermis, and senescence to understand these thickness and proliferation differences.

The impact of ASC treatment on dermis proteins was also studied. The negative control showed a clear decrease in procollagen III in the burn area on days 5, 10, and 15 which was not as clear in explant treated with ASCs. Indeed, the low intensity correlated with a lack of procollagen III was only visible on day 5 in explants treated with ASCs. Furthermore, statistical analysis highlighted this difference on day 15 between negative control and skins treated with EN-ASCs. These results suggest that ASCs, especially EN-ASCs, were involved in procollagen III synthesis and increased the dermal rate of procollagen III. However, the collagen III synthesis was surprisingly decreased on day 5 in MO and EN conditions compared to the negative control. This phenomenon could have been caused by the injection process which degraded the dermis, particularly with EN-. Indeed, the needle, although quite thin (0.80 mm), damaged the dermis damages and the microparticles which were around 500 µm in diameter created a hole in the dermis. Nevertheless, the level of collagen III returned to normal on day 10 and even increased on day 15 for explants treated with EN-ASCs. In addition, ASC treatment accelerated the kinetics of appearance of collagen I with a peak on day 10, but not its final rate. ASCs have an antifibrotic effect, which may explain the difference observed in collagen levels between the negative control and treated skins [61,62]. This property allows ASCs to regulate collagen production and prevent hypertrophic scar formation [63,64].

Thus, we demonstrated the impact of ASC treatment on collagens, but we did not obtain any results concerning myofibroblasts. Theoretically, ASCs should promote fibroblast conversion in myofibroblasts following (TGF)-β1 (Transforming Growth Factor β1) secretion [65] and through their angiogenic potential; however, we did not observe such an increase in the myofibroblast population. One of the hypotheses is that the burn model does not produce enough tension to mimic human skin in physiological conditions, thus allowing to observe any changes in myofibroblast rate.

For possible clinical application, it would be interesting to track ASCs in order to obtain data on the number of cells reaching the injured site, their viability, and the evolution of the capsules over time within the model. We also did not characterize the mechanical behavior of our microparticles after injection, which is an interesting point to investigate for the continuation of this study. To conclude, contrary to NaHS treatment, intradermal injection of human ASCs grown as a monolayer or encapsulated improved wound healing by accelerating re-epithelialization and collagen I synthesis; however, only the intradermal injection of human encapsulated ASCs accelerated keratinocyte migration and increased procollagen III and collagen III dermal rate in a second-degree burn model. This second-degree burn model on human skin provided results on the target treatments tested (hydrogel containing NaHS and ASC injection). This model allows testing treatments in conditions similar to a clinical application: either a topical application of a cream/gel/dressing or a dermal injection. This makes it easier to project results to a concrete clinical application of the treatment. We were able to obtain encouraging results in the use of encapsulated ASCs in the treatment of second-degree burns.

Supplementary Materials: The following are available online at https://www.mdpi.com/2673-1991/2/1/2/s1: Figure S1. Blow-up of epidermis restored post burn after treatment with poloxamer hydrogel containing NaHS on day 14 (0.25 mM–0.5 mM); Figure S2. Kinetics of α-SMA dermal expression in poloxamer hydrogel-treated ex vivo cultured human skin explants submitted to 10 s long experimental burn injury; Figure S3. Kinetics of collagen I dermal expression in poloxamer hydrogel-treated ex vivo cultured human skin explants submitted to 10 s long experimental burn injury; Figure S4. Kinetics of collagen III dermal expression in poloxamer hydrogel-treated ex vivo cultured human skin explants submitted to 10 s long experimental burn injury; Figure S5. Kinetics of HLA expression in poloxamer hydrogel-treated ex vivo cultured human skin explants submitted to 10 s long experimental burn injury; Figure S6. Kinetics of α-SMA dermal expression in ASCs-treated ex vivo cultured human skin explants submitted to 10 s long experimental burn injury; Figure S7. Kinetics of collagen III dermal expression in ASC-treated second-degree burn model; Figure S8. Kinetics of collagen I dermal expression in ASC-treated second-degree burn model.

Author Contributions: L.C., conceptualization, investigation, visualization, data curation, and writing (original draft preparation); O.G.-A., conceptualization, investigation, visualization, data curation, and writing (original draft preparation); M.C., investigation; M.-R.R., writing (review and editing); D.S., investigation and conceptualization; C.A., supervision, funding acquisition, and writing (review and editing). All authors have read and agreed to the published version of the manuscript.

Funding: This research was funded by a grant (C.A.) and a doctoral scholarship (to O.G.-A.) from the French Association for Research on Spa Waters (AFRETH: "Association Française pour la Recherche Thermale").

Institutional Review Board Statement: The study was conducted according to the guidelines of the Declaration of Helsinki and approved by the Institutional Review Board (or Ethics Committee) of Hospices Civils de Lyon. All the samples used in this study belong to a collection of human skin samples declared to the French research ministry (Declaration no. DC-2008-162 delivered to the Bank of Tissues and Cells of the Hospices Civils de Lyon).

Informed Consent Statement: Informed consent was obtained from all subjects involved in the study.

Acknowledgments: This research was also supported by the "Ministère de L'Education Nationale, L'Enseignement Supérieur et de la Recherche" and by INSERM, Hospices Civils de Lyon, University Claude Bernard Lyon-1. We wish to thank Bruno Chapuis from the CIQLE (Centre d'Imagerie Quantitative Lyon-Est, Faculté de médecine Lyon-Est, 69008, Lyon, France), who really helped us with image analysis and protein quantification.

Conflicts of Interest: The authors declare no conflict of interest.

References

1. Greenhalgh, D.G. Management of Burns. *N. Engl. J. Med.* **2019**, *380*, 2349–2359. [CrossRef]
2. Finnerty, C.C.; Jeschke, M.G.; Branski, L.K.; Barret, J.P.; Dziewulski, P.; Herndon, D.N. Hypertrophic scarring: The greatest unmet challenge following burn injury. *Lancet* **2016**, *388*, 1427–1436. [CrossRef]
3. Jeschke, M.G.; Shahrokhi, S.; Finnerty, C.C.; Branski, L.K.; Dibildox, M. Wound Coverage Technologies in Burn Care: Established Techniques. *J. Burn Care Res.* **2018**, *39*, 313–318. [CrossRef] [PubMed]
4. Saeidinia, A.; Keihanian, F.; Lashkari, A.P.; Lahiji, H.G.; Mobayyen, M.; Heidarzade, A.; Golchai, J. Partial-thickness burn wounds healing by topical treatment: A randomized controlled comparison between silver sulfadiazine and centiderm. *Medicine* **2017**, *96*, e6168. [CrossRef]
5. Wasiak, J.; Cleland, H.; Campbell, F.; Spinks, A. Dressings for superficial and partial thickness burns. *Cochrane Database Syst. Rev.* **2013**, *2013*. [CrossRef] [PubMed]
6. Auxenfans, C.; Menet, V.; Catherine, Z.; Shipkov, H.; Lacroix, P.; Bertin-Maghit, M.; Damour, O.; Braye, F. Cultured autologous keratinocytes in the treatment of large and deep burns: A retrospective study over 15 years. *Burns* **2015**, *41*, 71–79. [CrossRef]
7. Coolen, N.A.; Vlig, M.; van den Bogaerdt, A.J.; Middelkoop, E.; Ulrich, M.M.W. Development of an in vitro burn wound model. *Wound Repair Regen.* **2008**, *16*, 559–567. [CrossRef]
8. Emanuelsson, P.; Kratz, G. Characterization of a new in vitro burn wound model. *Burns* **1997**, *23*, 32–36. [CrossRef]
9. Qu, M.; Kruse, S.; Pitsch, H.; Pallua, N.; Nourbakhsh, M. Viability of human composite tissue model for experimental study of burns. *Discov. Med.* **2016**, *22*, 19–28. [PubMed]
10. Holzer, J.C.J.; Tiffner, K.; Kainz, S.; Reisenegger, P.; Bernardelli de Mattos, I.; Funk, M.; Lemarchand, T.; Laaff, H.; Bal, A.; Birngruber, T.; et al. A novel human ex-vivo burn model and the local cooling effect of a bacterial nanocellulose-based wound dressing. *Burns* **2020**. [CrossRef] [PubMed]
11. Sivamani, R.; Pullar, C.; Manabat-Hidalgo, C.; Rocke, D.; Carlsen, R.; Greenhalgh, D.; Isseroff, R. Stress-Mediated Increases in Systemic and Local Epinephrine Impair Skin Wound Healing: Potential New Indication for Beta Blockers. *PLoS Med.* **2009**, *6*, e1000012. [CrossRef] [PubMed]
12. Gross-Amat, O.; Guillen, M.; Salmon, D.; Nataf, S.; Auxenfans, C. Characterization of a Topically Testable Model of Burn Injury on Human Skin Explants. *Int. J. Mol. Sci.* **2020**, *21*, 6956. [CrossRef] [PubMed]
13. Balaji, S.; Moles, C.M.; Bhattacharya, S.S.; LeSaint, M.; Dhamija, Y.; Le, L.D.; King, A.; Kidd, M.; Bouso, M.F.; Shaaban, A.; et al. Comparison of interleukin 10 homologs on dermal wound healing using a novel human skin ex vivo organ culture model. *J. Surg. Res.* **2014**, *190*, 358–366. [CrossRef] [PubMed]

14. Tomic-Canic, M.; Mamber, S.W.; Stojadinovic, O.; Lee, B.; Radoja, N.; McMichael, J. Streptolysin O enhances keratinocyte migration and proliferation and promotes skin organ culture wound healing in vitro. *Wound Repair Regen.* **2007**, *15*, 71–79. [CrossRef] [PubMed]
15. Huang, A.; Seité, S.; Adar, T. The use of balneotherapy in dermatology. *Clin. Dermatol.* **2018**, *36*, 363–368. [CrossRef]
16. Carbajo, J.M.; Maraver, F. Sulphurous Mineral Waters: New Applications for Health. *Evid.-Based Complement. Altern. Med. ECAM* **2017**, *2017*, 8034084. [CrossRef]
17. Carubbi, C.; Gobbi, G.; Bucci, G.; Gesi, M.; Vitale, M.; Mirandola, P. Skin, Inflammation and Sulfurous Waters: What is Known, What is Believed. *Eur. J. Inflamm.* **2013**, *11*, 591–599. [CrossRef]
18. Gianfaldoni, S.; Tchernev, G.; Wollina, U.; Roccia, M.G.; Fioranelli, M.; Gianfaldoni, R.; Lotti, T. History of the Baths and Thermal Medicine. *Open Access Maced. J. Med. Sci.* **2017**, *5*, 566–568. [CrossRef]
19. Parihar, A.; Parihar, M.S.; Milner, S.; Bhat, S. Oxidative stress and anti-oxidative mobilization in burn injury. *Burns* **2008**, *34*, 6–17. [CrossRef]
20. Sahib, A.S.; Al-Jawad, F.H.; Al-Kaisy, A.A. Burns, Endothelial Dysfunction, and Oxidative Stress: The Role of Antioxidants. *Ann. Burns Fire Disasters* **2009**, *22*, 6–11. [PubMed]
21. Sahib, A.S.; Al-Jawad, F.H.; Alkaisy, A.A. Effect of Antioxidants on the Incidence of Wound Infection in Burn Patients. *Ann. Burns Fire Disasters* **2010**, *23*, 199–205.
22. Roshangar, L.; Soleimani Rad, J.; Kheirjou, R.; Reza Ranjkesh, M.; Ferdowsi Khosroshahi, A. Skin Burns: Review of Molecular Mechanisms and Therapeutic Approaches. *Wounds Compend. Clin. Res. Pract.* **2019**, *31*, 308–315.
23. Riyaz, N.; Arakkal, F.R. Spa therapy in dermatology. *Indian J. Dermatol. Venereol. Leprol.* **2011**, *77*, 128. [CrossRef]
24. Fazlzadeh, M.; Rostami, R.; Baghani, A.N.; Hazrati, S.; Mokammel, A. Hydrogen sulfide concentrations in indoor air of thermal springs. *Hum. Ecol. Risk Assess. Int. J.* **2018**, *24*, 1441–1452. [CrossRef]
25. Staffieri, A.; Abramo, A. Sulphurous-arsenical-ferruginous (thermal) water inhalations reduce nasal respiratory resistance and improve mucociliary clearance in patients with chronic sinonasal disease: Preliminary outcomes. *Acta Otolaryngol.* **2007**, *127*, 613–617. [CrossRef] [PubMed]
26. Viegas, J.; Esteves, A.F.; Cardoso, E.M.; Arosa, F.A.; Vitale, M.; Taborda-Barata, L. Biological Effects of Thermal Water-Associated Hydrogen Sulfide on Human Airways and Associated Immune Cells: Implications for Respiratory Diseases. *Front. Public Health* **2019**, *7*. [CrossRef]
27. Wang, Y.-D.; Li, J.-Y.; Qin, Y.; Liu, Q.; Liao, Z.-Z.; Xiao, X.-H. Exogenous Hydrogen Sulfide Alleviates-Induced Intracellular Inflammation in HepG2 Cells. *Exp. Clin. Endocrinol. Diabetes* **2020**, *128*, 137–143. [CrossRef] [PubMed]
28. Chen, X.; Liu, X. Hydrogen sulfide from a NaHS source attenuates dextran sulfate sodium (DSS)-induced inflammation via inhibiting nuclear factor-κB. *J. Zhejiang Univ. Sci. B* **2016**, *17*, 209–217. [CrossRef] [PubMed]
29. Perry, M.M.; Hui, C.K.; Whiteman, M.; Wood, M.E.; Adcock, I.; Kirkham, P.; Michaeloudes, C.; Chung, K.F. Hydrogen sulfide inhibits proliferation and release of IL-8 from human airway smooth muscle cells. *Am. J. Respir. Cell Mol. Biol.* **2011**, *45*, 746–752. [CrossRef]
30. Guan, R.; Wang, J.; Li, D.; Li, Z.; Liu, H.; Ding, M.; Cai, Z.; Liang, X.; Yang, Q.; Long, Z.; et al. Hydrogen sulfide inhibits cigarette smoke-induced inflammation and injury in alveolar epithelial cells by suppressing PHD2/HIF-1α/MAPK signaling pathway. *Int. Immunopharmacol.* **2020**, *81*, 105979. [CrossRef]
31. Li, P.; Guo, X. A review: Therapeutic potential of adipose-derived stem cells in cutaneous wound healing and regeneration. *Stem Cell Res. Ther.* **2018**, *9*, 302. [CrossRef]
32. Salgado, A.J.B.O.G.; Reis, R.L.G.; Sousa, N.J.C.; Gimble, J.M. Adipose tissue derived stem cells secretome: Soluble factors and their roles in regenerative medicine. *Curr. Stem Cell Res. Ther.* **2010**, *5*, 103–110. [CrossRef]
33. Kachgal, S.; Putnam, A.J. Mesenchymal stem cells from adipose and bone marrow promote angiogenesis via distinct cytokine and protease expression mechanisms. *Angiogenesis* **2011**, *14*, 47–59. [CrossRef]
34. Bertheuil, N.; Chaput, B.; Ménard, C.; Varin, A.; Laloze, J.; Watier, E.; Tarte, K. Adipose mesenchymal stromal cells: Definition, immunomodulatory properties, mechanical isolation and interest for plastic surgery. *Ann. Chir. Plast. Esthet.* **2019**, *64*, 1–10. [CrossRef]
35. Maria, A.T.J.; Toupet, K.; Maumus, M.; Fonteneau, G.; Le Quellec, A.; Jorgensen, C.; Guilpain, P.; Noël, D. Human adipose mesenchymal stem cells as potent anti-fibrosis therapy for systemic sclerosis. *J. Autoimmun.* **2016**, *70*, 31–39. [CrossRef]
36. De Becker, A.; Riet, I.V. Homing and migration of mesenchymal stromal cells: How to improve the efficacy of cell therapy? *World J. Stem Cells* **2016**, *8*, 73–87. [CrossRef] [PubMed]
37. Angoulvant, D.; Ivanes, F.; Ferrera, R.; Matthews, P.G.; Nataf, S.; Ovize, M. Mesenchymal stem cell conditioned media attenuates in vitro and ex vivo myocardial reperfusion injury. *J. Heart Lung Transplant.* **2011**, *30*, 95–102. [CrossRef] [PubMed]
38. Gnecchi, M.; Zhang, Z.; Ni, A.; Dzau, V.J. Paracrine mechanisms in adult stem cell signaling and therapy. *Circ. Res.* **2008**, *103*, 1204–1219. [CrossRef] [PubMed]

39. Ma, J.; Yan, X.; Lin, Y.; Tan, Q. Hepatocyte growth factor secreted from human adipose-derived stem cells inhibits fibrosis in hypertrophic scar fibroblasts. *Curr. Mol. Med.* **2020**. [CrossRef] [PubMed]
40. Capin, L.; Abbassi, N.; Lachat, M.; Calteau, M.; Barratier, C.; Mojallal, A.; Bourgeois, S.; Auxenfans, C. Encapsulation of Adipose-Derived Mesenchymal Stem Cells in Calcium Alginate Maintains Clonogenicity and Enhances their Secretory Profile. *Int. J. Mol. Sci.* **2020**, *21*, 6316. [CrossRef]
41. Gross-Amat, O.; Guillen, M.; Gimeno, J.-P.; Salzet, M.; Lebonvallet, N.; Misery, L.; Auxenfans, C.; Nataf, S. Molecular Mapping of Hydrogen Sulfide Targets in Normal Human Keratinocytes. *Int. J. Mol. Sci.* **2020**, *21*, 4648. [CrossRef] [PubMed]
42. Zhi, L.; Ang, A.D.; Zhang, H.; Moore, P.K.; Bhatia, M. Hydrogen sulfide induces the synthesis of proinflammatory cytokines in human monocyte cell line U937 via the ERK-NF-kappaB pathway. *J. Leukoc. Biol.* **2007**, *81*, 1322–1332. [CrossRef] [PubMed]
43. Zhang, J.; Sio, S.W.S.; Moochhala, S.; Bhatia, M. Role of hydrogen sulfide in severe burn injury-induced inflammation in mice. *Mol. Med. Camb. Mass* **2010**, *16*, 417–424. [CrossRef]
44. Li, L.; Bhatia, M.; Moore, P.K. Hydrogen sulphide—A novel mediator of inflammation? *Curr. Opin. Pharmacol.* **2006**, *6*, 125–129. [CrossRef]
45. Li, L.; Bhatia, M.; Zhu, Y.Z.; Zhu, Y.C.; Ramnath, R.D.; Wang, Z.J.; Anuar, F.B.M.; Whiteman, M.; Salto-Tellez, M.; Moore, P.K. Hydrogen sulfide is a novel mediator of lipopolysaccharide-induced inflammation in the mouse. *FASEB J.* **2005**, *19*, 1196–1198. [CrossRef] [PubMed]
46. Guo, L.; Peng, W.; Tao, J.; Lan, Z.; Hei, H.; Tian, L.; Pan, W.; Wang, L.; Zhang, X. Hydrogen Sulfide Inhibits Transforming Growth Factor-β1-Induced EMT via Wnt/Catenin Pathway. *PLoS ONE* **2016**, *11*, e0147018. [CrossRef]
47. Hellmich, M.R.; Szabo, C. Hydrogen Sulfide and Cancer. In *Chemistry, Biochemistry and Pharmacology of Hydrogen Sulfide. Handbook of Experimental Pharmacology*; Springer: Cham, Switzerland, 2015; Volume 230, pp. 233–241. [CrossRef]
48. Baskar, R.; Bian, J. Hydrogen sulfide gas has cell growth regulatory role. *Eur. J. Pharmacol.* **2011**, *656*, 5–9. [CrossRef]
49. Eberle, F.C.; Brück, J.; Holstein, J.; Hirahara, K.; Ghoreschi, K. Recent advances in understanding psoriasis. *F1000Research* **2016**, *5*. [CrossRef] [PubMed]
50. Danilenko, D.M. An Overview of the Pathogenesis of Immune-mediated Skin Injury. *Toxicol. Pathol.* **2016**, *44*, 536–544. [CrossRef]
51. Ud-Din, S.; Bayat, A. Non-animal models of wound healing in cutaneous repair: In silico, in vitro, ex vivo, and in vivo models of wounds and scars in human skin. *Wound Repair Regen.* **2017**, *25*, 164–176. [CrossRef]
52. Daryabeigi, R.; Heidari, M.; Hosseini, S.A.; Omranifar, M. Comparison of healing time of the 2nd degree burn wounds with two dressing methods of fundermol herbal ointment and 1% silver sulfadiazine cream. *Iran. J. Nurs. Midwifery Res.* **2010**, *15*, 97–101. [PubMed]
53. Mojallal, A.; Lequeux, C.; Shipkov, C.; Rifkin, L.; Rohrich, R.; Duclos, A.; Brown, S.; Damour, O. Stem cells, mature adipocytes, and extracellular scaffold: What does each contribute to fat graft survival? *Aesthetic Plast. Surg.* **2011**, *35*, 1061–1072. [CrossRef] [PubMed]
54. de Vos, P.; Lazarjani, H.A.; Poncelet, D.; Faas, M.M. Polymers in cell encapsulation from an enveloped cell perspective. *Adv. Drug Deliv. Rev.* **2014**, *67–68*, 15–34. [CrossRef]
55. De Vos, P.; Hoogmoed, C.G.; Busscher, H.J. Chemistry and biocompatibility of alginate-PLL capsules for immunoprotection of mammalian cells. *J. Biomed. Mater. Res.* **2002**, *60*, 252–259. [CrossRef] [PubMed]
56. Orive, G.; Ponce, S.; Hernández, R.M.; Gascón, A.R.; Igartua, M.; Pedraz, J.L. Biocompatibility of microcapsules for cell immobilization elaborated with different type of alginates. *Biomaterials* **2002**, *23*, 3825–3831. [CrossRef]
57. Puissant, B.; Barreau, C.; Bourin, P.; Clavel, C.; Corre, J.; Bousquet, C.; Taureau, C.; Cousin, B.; Abbal, M.; Laharrague, P.; et al. Immunomodulatory effect of human adipose tissue-derived adult stem cells: Comparison with bone marrow mesenchymal stem cells. *Br. J. Haematol.* **2005**, *129*, 118–129. [CrossRef]
58. McIntosh, K.R. Evaluation of cellular and humoral immune responses to allogeneic adipose-derived stem/stromal cells. In *Adipose-Derived Stem Cells. Methods in Molecular Biology*; Humana Press: Totowa, NJ, USA, 2011; Volume 702, pp. 133–150. [CrossRef]
59. Hassan, W.U.; Greiser, U.; Wang, W. Role of adipose-derived stem cells in wound healing. *Wound Repair Regen.* **2014**, *22*, 313–325. [CrossRef]
60. Saito, Y.; Shimada, M.; Utsunomiya, T.; Ikemoto, T.; Yamada, S.; Morine, Y.; Imura, S.; Mori, H.; Arakawa, Y.; Kanamoto, M.; et al. Homing effect of adipose-derived stem cells to the injured liver: The shift of stromal cell-derived factor 1 expressions. *J. Hepato-Biliary-Pancreat. Sci.* **2014**, *21*, 873–880. [CrossRef]
61. Deng, J.; Shi, Y.; Gao, Z.; Zhang, W.; Wu, X.; Cao, W.; Liu, W. Inhibition of Pathological Phenotype of Hypertrophic Scar Fibroblasts Via Coculture with Adipose-Derived Stem Cells. *Tissue Eng. Part A* **2018**, *24*, 382–393. [CrossRef]
62. Zarei, F.; Abbaszadeh, A. Stem cell and skin rejuvenation. *J. Cosmet. Laser Ther.* **2018**, *20*, 193–197. [CrossRef] [PubMed]
63. Bliley, J.M.; Argenta, A.; Satish, L.; McLaughlin, M.M.; Dees, A.; Tompkins-Rhoades, C.; Marra, K.G.; Rubin, J.P. Administration of adipose-derived stem cells enhances vascularity, induces collagen deposition, and dermal adipogenesis in burn wounds. *Burns* **2016**, *42*, 1212–1222. [CrossRef] [PubMed]

64. Domergue, S.; Bony, C.; Maumus, M.; Toupet, K.; Frouin, E.; Rigau, V.; Vozenin, M.-C.; Magalon, G.; Jorgensen, C.; Noël, D. Comparison between Stromal Vascular Fraction and Adipose Mesenchymal Stem Cells in Remodeling Hypertrophic Scars. *PLoS ONE* **2016**, *11*, e0156161. [CrossRef] [PubMed]
65. Leonov, Y.I.; Shkumat, M.S.; Klymenko, P.P.; Hovorun, M.Y.; Guzyk, M.M.; Kuchmerovska, T.M.; Pishel, I.M. Effect of insulin-like growth factor transgene on wound healing in mice with streptozotocin-induced diabetes. *Cytol. Genet.* **2015**, *49*, 19–26. [CrossRef]